Nonlinear Full-Process Shear Analysis of RC Structural Members Using Planar Membrane Element: Implementation and Application

Meng Zhou[1,2], *Jian-Guo Nie*[1,2], *and Jian-Sheng Fan*[1,2]

[1]Key Laboratory of Civil Engineering Safety and Durability of China Education Ministry, Beijing, 100084, China;
[2]Department of Civil Engineering, Tsinghua University, Beijing, 100084, China;
email: zhoum07@mails.tsinghua.edu.cn

ABSTRACT

Numerical stability and computational accuracy is required for the nonlinear full-process shear analysis of reinforced concrete (RC) structures and members. For this requirement, the planar membrane element is implemented and employed based on the rotating crack model. First, the complex plane stress conditions of RC members are classified into three groups of principle strain states in the principle strain space. Then, the computational methods for the three different principle strain states to update stress and calculate Jacobian Matrix are given. Third, the flowchart for programming is developed and the program of the planar membrane element is implemented based on the large generic finite element package ABAQUS 6.9. Finally, tests of a group of classic RC beam and a series of typical RC shear wall are selected for the application and validation. Good agreement is found between the test and predicted curves and ultimate capacities. Comparison results also demonstrate that, by integrating the flowchart given in this paper into the program of the planar membrane element, good numerical stability and computational accuracy can be gained.

INTRODUCTION

Focused on the nonlinear shear behavior of concrete, a critical problem in researches of reinforced concrete (RC) structures, five rational analytical models have been proposed over the past three decades. These models are the modified compression field theory (MCFT) (Vecchio and Collins 1986), the rotating-angle softened-truss model (RA-STM) (Hsu 1991; Hsu 1993; Belarbi and Hsu 1994 and 1995; Pang and Hsu 1995; Hsu and Zhang 1996), the fixed-angle softened-truss model (FA-STM) (Pang and Hsu 1996; Hsu and Zhang 1997), the disturbed stress field model (DSFM) (Vecchio 2000 and 2001; Vecchio et al. 2001), and the softened membrane model (SMM) (Zhu, Hsu and Lee 2001; Zhu and Hsu 2002; Hsu and Zhu 2002). In the implementation and application of these rotating crack models, good numerical stability and computational accuracy is required, since the structural members and structures, like tube structures, walls and beams, are usually consisted of hundreds or thousands of RC elements, which are in different mechanical states or

different stress-strain conditions, as shown in Figure 1.

In this paper, to gain proper numerical stability and computational accuracy, all the six different plane stress conditions illustrated in Figure 1 are characterized by three kinds of principle strain states: double-tension (DT), tension-compression (TC) and double-compression (DC). The calculating of different principle strain states is finely considered in the program of planar membrane element (PME). The PME is a kind of element used in the finite element analysis (FEA), consisted of concrete and rebar, as shown in Figure 1.

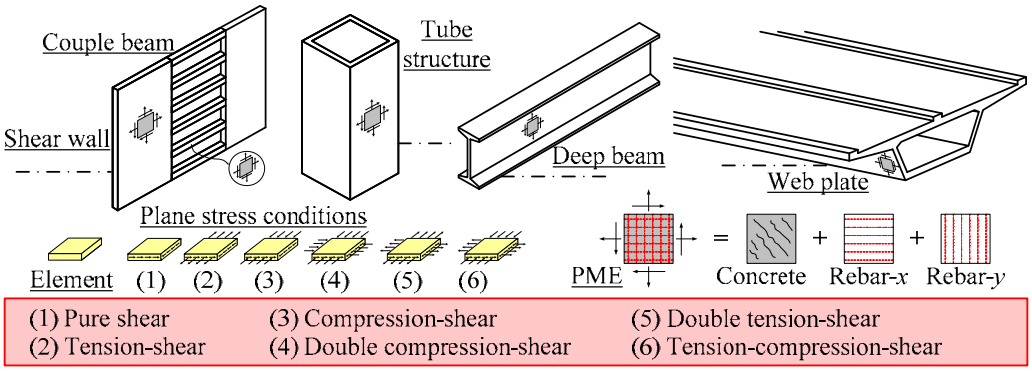

Figure 1. Different plane stress conditions of RC structures

IMPLEMENTATION

Constitutive laws. Typical rotating crack models consist of three groups of equations, including the compatibility equations, constitutive laws and equilibrium equations. The compatibility equations can be summarized into Eq.1 in vector-matrix form. $\boldsymbol{E_{xy}}$ is the strain vector of PME in the *x*-*y* coordinate system and equals $(\varepsilon_x, \varepsilon_y, \gamma_{xy}/2)^T$, while $\boldsymbol{E_{12}}$,which equals $(\varepsilon_1, \varepsilon_2, \gamma_{12}/2)^T$, is the strain vector in the principle strain space. $\boldsymbol{T(-\theta)}$ is the transformation matrix, and θ is the principle strain direction angle. Eq. 2 expresses the equilibrium equations in vector-matrix term. $\boldsymbol{S_{xy}}$ is the stress vector of PME in the *x*-*y* system and equals $(f_x, f_y, v_{xy})^T$. $\boldsymbol{S_{cxy}}$ and $\boldsymbol{S_{rxy}}$ is the stress of the concrete and rebar in the x-y system and equals $(f_{cx}, f_{cy}, v_{cxy})^T$ and $(f_{rx}, f_{ry}, 0)^T$, respectively. $\boldsymbol{S_{c12}}$, which equals $(f_{c1}, f_{c2}, v_{c12})^T$, is the stress of the concrete and rebar in the principle strain space, respectively. The definition of the principle strain direction angle and detailed deviation of compatibility and equilibrium equations are given by Nie and Zhou (2013). It is worthwhile to know that the selection of the constitutive laws is important to gain computational accuracy and numerical stability. Based on previous studies of Vecchio and Collins (1986) and Nie and Zhou (2013), the constitutive laws illustrated in Figure 2 are selected in this paper for the implementation of PME. Notably, in the concrete compressive law, the residual concrete compression stress is set to be 10 percent of its ultimate compressive strength. This is a practical way to improve the numerical stability of PME while brings few effect on computational accuracy.

$$\boldsymbol{E}_{xy} = \boldsymbol{T}(-\boldsymbol{\theta})\cdot\boldsymbol{E}_{12} \quad \text{Eq. 1}$$

$$\boldsymbol{S}_{xy} = \boldsymbol{S}_{cxy}+\boldsymbol{S}_{rxy} = \boldsymbol{T}(-\boldsymbol{\theta})\cdot\boldsymbol{S}_{c12} + \boldsymbol{S}_{rxy} \quad \text{Eq. 2}$$

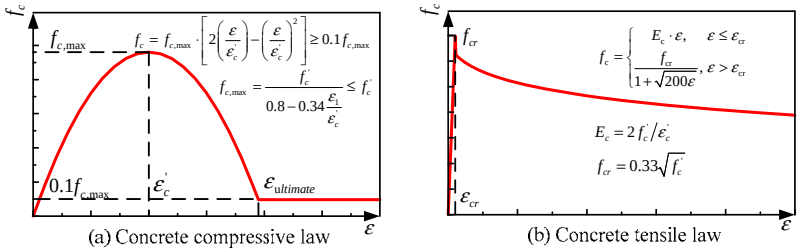

Figure 2. Constitutive laws for concrete

Through the three groups of equations mentioned above, the stress vector $\boldsymbol{S}_{xy}$ can be calculated and updated in every iteration of PME with given stress strain vector $\boldsymbol{E}_{xy}$. But to accomplish a complete iteration, another character is essential, the Jocobian Matrix $\boldsymbol{D}$. Simplified from the formulas of Nie and Zhou (2013), Eq. 3 gives out the formulas for the calculation of $\boldsymbol{D}$.

$$\boldsymbol{D} = \boldsymbol{T}(-\boldsymbol{\theta})\cdot\boldsymbol{D}_{c,12}\cdot\boldsymbol{T}(-\boldsymbol{\theta}) + \boldsymbol{D}_{r,xy} \quad \text{Eq. 3}$$

in which, $\boldsymbol{D}_{c,12}=\begin{pmatrix} \frac{\partial f_{c1}}{\partial \varepsilon_1} & \frac{\partial f_{c1}}{\partial \varepsilon_2} & 0 \\ \frac{\partial f_{c2}}{\partial \varepsilon_1} & \frac{\partial f_{c2}}{\partial \varepsilon_2} & 0 \\ 0 & 0 & \frac{f_{c1}-f_{c2}}{\varepsilon_1-\varepsilon_2} \end{pmatrix}$ and $\boldsymbol{D}_{r,xy}=\begin{pmatrix} \rho_{rx}\cdot\frac{\partial f_{rx}}{\partial \varepsilon_x} & 0 & 0 \\ 0 & \rho_{ry}\cdot\frac{\partial f_{ry}}{\partial \varepsilon_y} & 0 \\ 0 & 0 & 0 \end{pmatrix}$

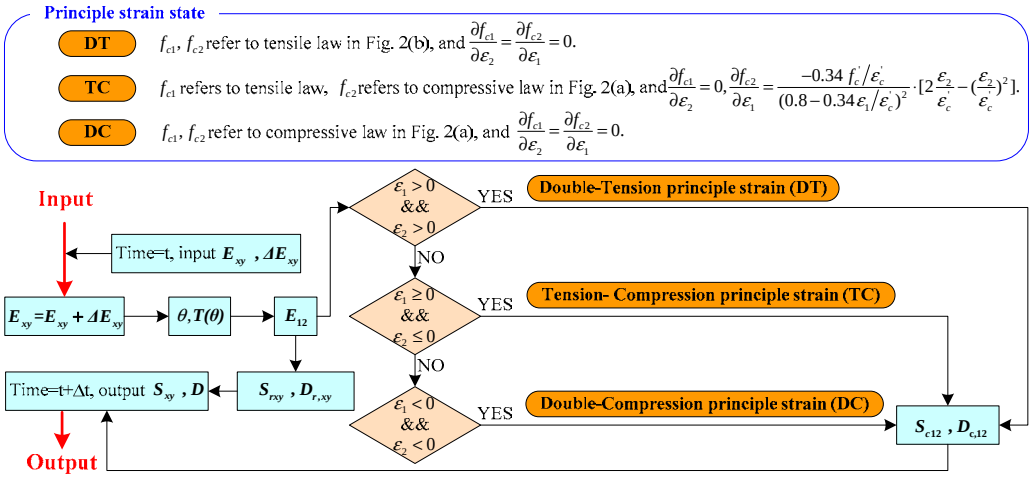

Figure 3. Flowchart for the programming of PME

Programming. Figure 3 shows the flowchart for the programming of PME. The current element strain vector and strain increment vector is input from the main program of ABAQUS. The purpose for the program of PME is to update and output the element stress vector and Jocobian Matrix to the main program for the next

iteration. Three kinds of principle strain states, including DT, TC and DC, are distinguished in Figure3. Details for calculating of the Jocobian Matrix for different principle strain states are illustrated, respectively.

APPLICATION

Classic RC beam tests. The 12 beams tested by Bresler and Scordelis (1962) consist of four series of three beams; each series differs in amount of longitudinal rebar, amount of stirrups, span length, cross-section dimensions and concrete strength. The beams tested also cover a range of failure modes: diagonal-tension (D-T), shear-compression (V-C) and flexure-compression (F-C). Table 1 gives the details of the beams. The yield strength of Rebar ϕ 6.4, ϕ 12.7 and ϕ 28.7 is 325, 345 and 555 MPa, respectively.

Table 1. Details of Bresler-Scordelis beams

Beam number	f_c' (MPa)	b (mm)	h (mm)	d (mm)	Span (mm)	Bottom rebar	Top rebar	Stirrups
OA1	22.6	310	556	461	3660	4ϕ28.7	—	—
OA2	23.7	305	561	466	4570	5ϕ28.7	—	—
OA3	37.6	307	556	462	6400	6ϕ28.7	—	—
A1	24.1	307	561	466	3660	4ϕ28.7	2ϕ12.7	ϕ6.4 @210
A2	24.3	305	559	464	4570	5ϕ28.7	2ϕ12.7	ϕ6.4 @210
A3	35.1	307	561	466	6400	6ϕ28.7	2ϕ12.7	ϕ6.4 @210
B1	24.8	231	556	461	3660	4ϕ28.7	2ϕ12.7	ϕ6.4 @210
B2	23.2	229	561	466	4570	4ϕ28.7	2ϕ12.7	ϕ6.4 @210
B3	38.8	229	556	461	6400	5ϕ28.7	2ϕ12.7	ϕ6.4 @210
C1	29.6	155	559	464	3660	2ϕ28.7	2ϕ12.7	ϕ6.4 @210
C2	23.8	152	559	464	4570	4ϕ28.7	2ϕ12.7	ϕ6.4 @210
C3	35.1	155	554	459	6400	4ϕ28.7	2ϕ12.7	ϕ6.4 @210

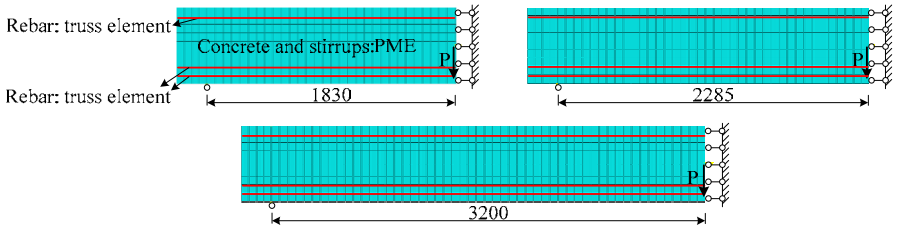

Figure 4 Typical FE meshes for Bresler-Scordelis beams

The FE analysis is performed using the large generic FE package ABAQUS. The typical finite element meshes used to simulate the Bresler-Scodelis beams are shown in Figure 4. All longitudinal rebar is modeled using truss element; all stirrups are modeled as smeared reinforcement with concrete using PME. The concrete tension strength is estimated as $0.3(f_c')^{0.5}$.

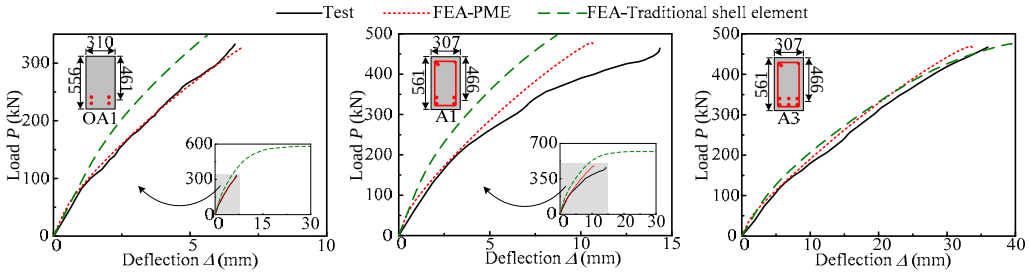

Figure 5 Load-deflection curves of Beam OA1/A1/A3

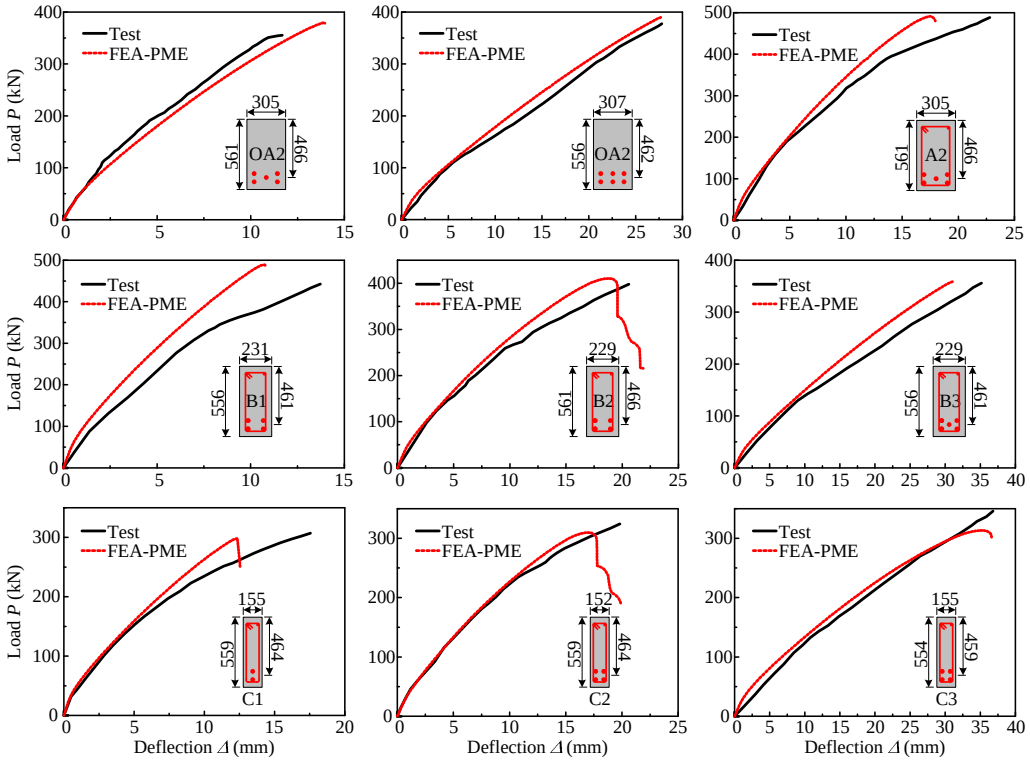

Figure 6 Load-deflection curves of Bresler-Scordelis beams

The Bresler-Scordelis beams are characterized by three different failure modes: D-T for Beam OA1/OA2/OA3, V-C for Beam A1/A2/B1/B2/C1/C2, and F-C for Beam A3/B3/C3. Fig 5 compares the test with the FEA results using PME and traditional shell element of Beam OA1/A1/A3, each specimen represents a typical failure mode. Comparison result demonstrates that the predicted curves for Beam OA1 and A1 using traditional shell element show unexpected good ductility performance and are significantly higher than those using PME, which agree well with the test curves. This result may be caused by the overestimation of concrete shear strength while using traditional shell element, since fixed crack model is employed in the traditional shell element and its shear transfer coefficient is constantly positive. Hence the shear capacity of the beam is overestimated and

continually increases as the load procedure processing on. When the overestimated shear capacity exceeds the flexure capacity of the beam, its failure mode turns in to F-C, which is of good ductility performance. This can be further validated by the comparison result of Beam A3: test curve agrees well with both predicted curves using PME and traditional shell element since the failure mode of Beam A3 itself is F-C and the shear overestimation brings no change to its failure mode. Fig 6 shows the comparison results of other 9 beams. All comparison results demonstrate good computational accuracy of predicted curves using PME. Proper numerical stability is also shown during the simulating of these four series beams covering a wide range of failure modes.

Typical RC shear wall tests. The RC shear wall is consisted of the RC wall and side column. The 6 RC shear walls tested by Sun (2007) cover a range of the amount of distributed rebar, amount of side column reinforcement, and amount of side column stirrups. Since the side column of Wall SRCW3 uses concrete filled steel tube and its confine effect cannot be considered by PME currently, the specimen is not included in the validation. Table 2 gives the cross-section details of Sun walls. The yield strength of Rebar ϕ 6, ϕ 8, ϕ 12, ϕ 16, ϕ 20 and ϕ 22 is 285, 300, 387, 436, 442 and 445 MPa, respectively. The yield strength of the I-shape steel used in Wall SRCW2 is 345 MPa.

Table 2. Cross-section details of Sun walls

Wall number	Ratios of distributed rebar		Side column rebar	Side column stirrups	Side column steel
	Horizontal	Vertical			
SRCW1	0.35%	0.35%	6ϕ16	ϕ6@70	—
SRCW2	0.35%	0.35%	6ϕ16	ϕ6@70	I4×50×40
SRCW4	0.35%	0.35%	6ϕ16+4ϕ12	ϕ6@70+ϕ6@70	—
SRCW5	0.35%	0.35%	6ϕ20	ϕ8@70	—
SRCW6	1.26%	1.26%	6ϕ22	ϕ8@70	—

Figure 7 illustrates FE meshes of Sun walls, also with the geometry details. For the RC wall section, distributed rebar in both vertical and horizontal directions are modeled as smeared reinforcement with concrete using PME. For the side column section, rebar and steel is approximately modeled like stirrups as smeared reinforcement with concrete using PME. The horizontal loading equipment is 200mm in height, so the loading center is 100mm above the wall, as shown in Figure 7.

All the 5 Sun walls show the same failure mode in the test: diagonal-tension (D-T). Figure 8 compares the test and predicted ultimate capacity and horizontal load-displacement skeleton curves. It is demonstrated that the predicted initial stiffness agrees well with the test. Good agreement between the test and predicted ultimate capacity is observed, with an average error of 4%. The Sun walls can be simulated by FE models using PME, with proper computational accuracy and numerical stability.

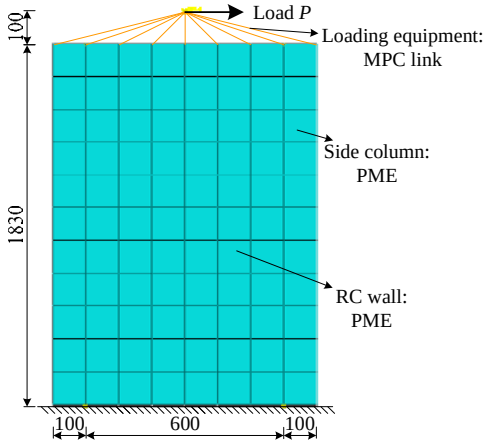

Figure 7. FE meshes of Sun walls

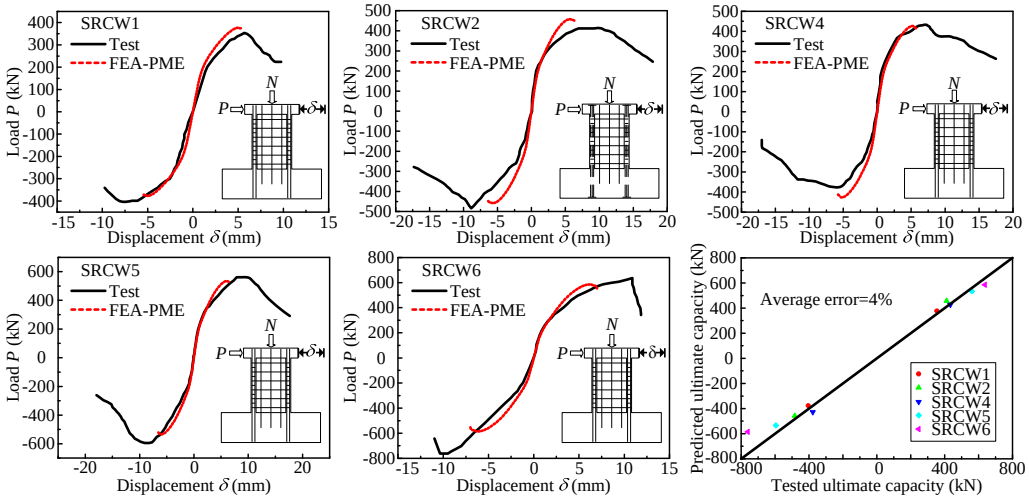

Figure 8. Comparison of test and predicted results of Sun walls

CONCLUSION

In this paper, the planar membrane element (PME) is implemented for the nonlinear full-process shear analysis of RC structural members subjected to compression, flexure and shear based on the rotating crack model. Detailed flowchart for programming of PME is developed for proper numerical stability and computational accuracy. A group of classic RC beams tests and a series of typical RC shear walls tests are selected, modeled and analyzed using PME. It is concluded that detailed considering of three principle strain states would strengthen the numerical stability during the FE analysis of structural members under complex mechanical conditions, and that the proposed PME possesses good computational accuracy and high analyzing efficiency in simulating RC structural members.

ACKNOWLEDGEMENT

The writers gratefully acknowledge the financial support provided by the National Science Fund of China (51138007), the National Science & Technology Support Program of China (2011BAJ09B01), and the National Science & Technology Support Program of China (2011BAJ09B02)

REFERENCES

Belarbi A. and Hsu T. T. C. (1994). "Constitutive laws of concrete in tension and reinforcing bars stiffened by concrete." *ACI Structural Journal*, 91(4), 465-474.

Belarbi A. and Hsu T. T. C. (1995). "Constitutive laws of softened concrete in biaxial tension-compression." *ACI Structural Journal*, 92(5), 562-573.

Bresler B. and Scordelis A. C. (1962). "Shear Strength of Reinforced Concrete Beams." *ACI Structural Journal*, 60(1), 51-72.

Hsu T. T. C. (1991). "Nonlinear analysis of concrete membrane elements." *ACI Structural Journal*, 88(5), 552-561.

Hsu T. T. C. (1993). *Unified theory of reinforced concrete*, CRC Press Inc., Boca Raton, Fla., 336-337.

Hsu T. T. C. and Zhang L. X. (1996). "Tension stiffening in reinforced concrete membrane elements. " *ACI Structural Journal*, 93(1), 108-115.

Hsu T. T. C. and Zhang L. X. (1997). "Nonlinear analysis of membrane elements by fixed-angle softened-truss model." *ACI Structural Journal*, 94(5), 483-492.

Hsu T. T. C. and Zhu R. R. H. (2002). "Softened membrane model for reinforced concrete elements in shear." *ACI Structural Journal*, 99(4), 460-469.

Nie J. G. and Zhou M. (2013). "A planar membrane element for nonlinear shear analysis of steel-concrete composite structures based on modified compression-field theory." China Civil Engineering Journal, 46(9), 62-71.

Pang X. B. and Hsu T. T. C. (1995). "Behavior of reinforced concrete membrane elements in shear." *ACI Structural Journal*, 92(6), 665-677.

Pang X. B. and Hsu T. T. C. (1996). "Fixed angle softened truss model for reinforced concrete." *ACI Structural Journal*, 93(2), 197-207.

Sun J. C. (2007). "Study on Shear Behavior and Design Method of Steel-Concrete Composite Wall for High-Rise Building." PhD thesis, *China Academy of Building Research*, Beijing (in Chinese).

Vecchio F. J. and Collins M. P. (1986). "The modified compression-field theory for reinforced concrete elements subjected to shear." *ACI Structural Journal*, 83(2), 219-231.

Vecchio F. J. (2000). "Disturbed stress field model for reinforced concrete: Formulation." *J. Struct. Engrg.*, ASCE, 126(9), 1070-1077.

Vecchio F. J. (2001). "Disturbed stress field model for reinforced concrete: Implementation." *J. Struct. Engrg.*, ASCE, 127(1), 12-20.

Vecchio F. J., Lai D., Shim W. and Ng J. (2001). "Disturbed stress field model for reinforced concrete: Validation." *J. Struct. Engrg.*, ASCE, 127(4), 350-358.

Zhu R. R. H., Hsu T. T. C. and Lee J. Y. (2001). "Rational shear modulus for smeared-crack analysis of reinforced concrete." *ACI Structural Journal*, 98(4), 443-450.

Zhu R. R. H. and Hsu T. T. C. (2002). "Poisson effect in reinforced concrete membrane elements." *ACI Structural Journal*, 99(5), 631-640.